Int. J. Electrochem. Sci., 11 **(2016)** 9881 – 9890, doi: 10.20964/2016.12.08

International Journal of
ELECTROCHEMICAL
SCIENCE
www.electrochemsci.org

Synthesis of N-doped carbon by microwave-assisited pyrolysis ionic liquid for lithium-ion batteries

Yanshuang Meng[1,2], *Jun Xia*[1], *Fuliang Zhu*[1,2,*], *Yue Zhang*[3,*]

[1] School of Materials Science and Engineering, Lanzhou University of Technology, Lanzhou 730050,China
[2] State Key Laboratory of Advanced Processing and Recycling of Non-ferrous Metals， Lanzhou 730050,China
[3] Department of Industrial Engineering, Texas Tech University, Lubbock, Texas, 79409, USA)
[*]E-mail: chzfl@126.com, yue.zhang@ttu.edu

Received: 26 August 2016 / *Accepted:* 17 October 2016 / *Published:* 10 November 2016

Nitrogen-doped carbon (NDC) was prepared by a novel microwave-assisted pyrolysis of ionic liquid method. The carbonation temperature and time of the ionic liquid were obviously dropped down by microwave-assisted pyrolysis. The results of XRD, Raman spectra and FT-IR spectra indicated that the pyrolysis product was graphitic nitrogen-doped carbon. The nitrogen dopant in NDC created a porous structure and a large number of defects, which introduced many active sites for the Li^+ ion adsorption. Consequently, the NDC delivered high electrochemical performances when used as anode for lithium ion batteries. The NDC electrode exhibited a specific capacity of 243.6mAh.g^{-1} after 50 cycles at 0.2C and 196mAh.g^{-1} after 50 cycles at 1.0C.

Keywords: Nitrogen-doped carbon, Microwave-assisted pyrolysis, Ionic liquid

1. INTRODUCTION

Lithium-ion batteries (LIBs) have been identified as one of the most important energy storage device, as their applications are successfully expanding from small-scale portable electronics to large-scale electronic vehicles[1] . Previous researches revealed that the electrochemical properties of electrode materials, especially the anode material, can largely determine the performance of LIBs[2, 3]. The nanostructured carbon is one of the core materials for high performance energy storage devices since it possesses many ideal properties as anode materials, like high conductivity, high specific surface area and high chemical stability. Numerous of studies have been carried out to improve the electrochemical properties by increase the surface area and electrical conductivity of anode

materials[4-6] . Another method, which improves the electrochemical properties for the carbon-based electrode by doping heteroatoms into carbon framework, has been investigated to a lesser extend but are gaining increased interest recently. The presence of heteroatoms, such as nitrogen, in the carbon framework can enhance the electrode/electrolyte wettability, the reactivity, the electronical conductivity and, therefore, the electrochemical performance[2, 7-9] . The preparation of nitrogen-doped carbon can be divided into in-situ doping method and post-treatment method. Nitrogen-containing organics are usually used as carbon sources in in-situ doping method[10-13] . In the in-situ method, the nitrogen-containing carbon precursors are usually used, of which the nitrogen atoms are incorporated into carbon frames after the pyrolysis process. In the post-treatment method, the nitrogen-containing organic group is grafted onto the surface of the as-prepared carbon frame after treatment in nitrogen-containing gas, such as nitrogen or ammonia, at high temperature[14-19] . One drawback of the post-treatment method is the low doping content of nitrogen, which can be overcome by in-situ pyrolysis of nitrogen-rich carbon precursors[20].

Recently, ionic liquids (ILs) have been the focus of an ever increasing amount of research as the carbon precursors due to its extraordinary properties, such as negligible vapor pressure and structure designability[21-24] . The negligible vapor of ILs enable them simple processing and shaping during the carbonization process without evaporation. Moreover, as the ILs are designable, it is feasible to synthesis carbon materials with controllable structure and a certain amount of heteroatoms by adjusting the cation or anion components of ILs. Due to these unique properties, almost all IL-derived carbons contained higher doping contents of nitrogen when compared with the carbon materials prepared by other nitrogen-containing carbon precursors[25]. For this reason, ILs are preferred to be used as the carbon precursors of the electrode materials of LIBs since the doped nitrogen atoms can create more defect and edge site that are active for the Li^+ ion adsorption, which can improve the performance of LIBs. Lee et.al empoyed ILs with anion-containing nitrile groups, such as [EMIm][$C(CN)_3$], [BMIm][$C(CN)_3$] and [BCNIm][$C(CN)_3$], as carbon precursor and prepared nitrogen-doped carbon[26]. The work showed that nitrogen content of carbon materials was closely related to the type and the pyrolysis temperature of the ILs. Fulvio and co-workers used a mixture of two different ILs ,[BMIm][$C(CN)_3$] and [EMIm][$B(CN)_4$], as carbon precursor to prepare nitrogen-doped carbon materials[24]. Nitrogen-doped carbon materials with different structure and morphology were obtained by adjusting the pyrolysis temperature of ILs and the ratio of two ILs.

However, all the reported nitrogen-doped carbon materials were produced by flame heating process, which has the disadvantages of high pyrolysis temperature of about 800°C and long pyrolysis time of several hours. As an increasing pyrolysis temperature always results in a decrease of nitrogen content, it is critical to explore a method that could complete the process at a relatively low temperature at a fast speed[5, 25] .

Microwave-assisted synthesis has attracted tremendous attention as its successful applications in fabrication and modification of carbon nanomaterials. The microwave-heating technology possesses the advantages of fast heating rate, material-selective heating, contactless heating, and instantaneous on/off switching of heating. These special properties make it possible to synthesis nitrogen-doped carbon materials at a low temperature in a shorter time, which lead to an energy and time saving process and might even suppress undesired side-reactions and enable new reaction pathways[27, 28] .

In this work, we have produced the nitrogen-doped carbon (NDC) at low temperature by using microwave-assisted pyrolysis ILs. The pyrolysis product NDC was first characterized by a variety of techniques including FT-IR, XRD, XPS, Raman spectra, TEM and EDS to determine the quality of the pyrolysis product. The NDC was fabricated as the anode electrode of a LIBs and characterized to measure the electrochemical properties. It was found that the NDC has excellent electrochemical performance.

2. EXPERIMENTAL

2.1 Preparation of nitrogen-doped carbon

The ionic liquid 1-butyl-3-methylimidazolium dicyanamide [BMIm]$N(CN)_2$ was purchased from Lanzhou Institute of Chemical Physics and used without further purification. [BMIm]$N(CN)_2$ was loaded into a quartz boat, which was put into HAMiLab-V1500 microwave sintering furnace (Synotherm Corporation) and heated to 500 °C in a nitrogen atmosphere with 800W. The pyrolysis product, nitrogen-doped carbon, was denoted as NDC.

2.2 Structural and Morphology Characterization

Fourier transform infrared (FT-IR) spectra were recorded on a Jasco-680 (Japan) spectrophotometer. The spectra of solids were carried out using KBr pellets. Raman spectra were recorded on a LabRAM HR UV/vis/NIR (Horiba Jobin Yvon, France) using a CW Ar-ion laser (514.5 nm) as an excitation source. X-ray diffraction (XRD) characterization of the samples was performed with a Rigaku D/MAX 2500V X-ray diffractometer and filtered Cu Kα radiation. X-ray photoelectron spectroscopy (XPS) was recorded using a Kratos XSAM 800 spectrometer (Manchester, UK). Field-emission scanning electron microscopy (FT-SEM) was carried out with a JEOL-7500F microscope equipped with an energy-dispersive spectroscopy (EDS) instrument. Transmission electron microscopy (TEM) characterizations were carried out with a JEOL JEM-2010F equipment. The N_2 adsorption–desorption isotherm was obtained using an N_2 adsorption analyzer (Autosorb-IQ2-MP-C system). The specific surface area of NDC was calculated by BET method.

2.3 Electrochemical Characterization

Electrochemical measurements were performed using a coin-type cell (model 2032). The anode electrodes were fabricated by dispersing 85 wt% active material NDC, 8 wt% Super P, and 7 wt% polyvinylidene fluoride in nmethyl pyrrolidone to form a slurry. The slurry was then coated onto a Cu foil, and the solvent was evaporated at 90 °C for 12 h in vacuum. A lithium foil was invoked as counter electrode. The separator between the electrodes was Celgard2400 micro-porous polypropylene film. The electrolyte used was a solution of 1 M lithium hexafluorophosphate ($LiPF_6$) in a mixture of ethylene carbonate (EC): diethyl carbonate (DEC) with a volume ratio of 1: 1. Coin cell was assembled

inside the glove box filled with dry argon. Land CT2001D was used for the analysis of cell performance by constant charge-discharge testing.

3. RESULTS AND DISCUSSION

The temperatures during microwave irradiation were recorded per minute and the pyrolysis products from selected temperatures were weighted. The temperature-rising and mass loss of $[BMIm]N(CN)_2$ during microwave irradiation was shown in Figure 1. There were three maximum mass losses (M_1, M_2 and M_3) arose at 150 °C, 320 °C and 445 °C, respectively. They were significantly lower than the maximum mass losses at 316 °C, 398 °C and 492 °C under flame heating process[29].

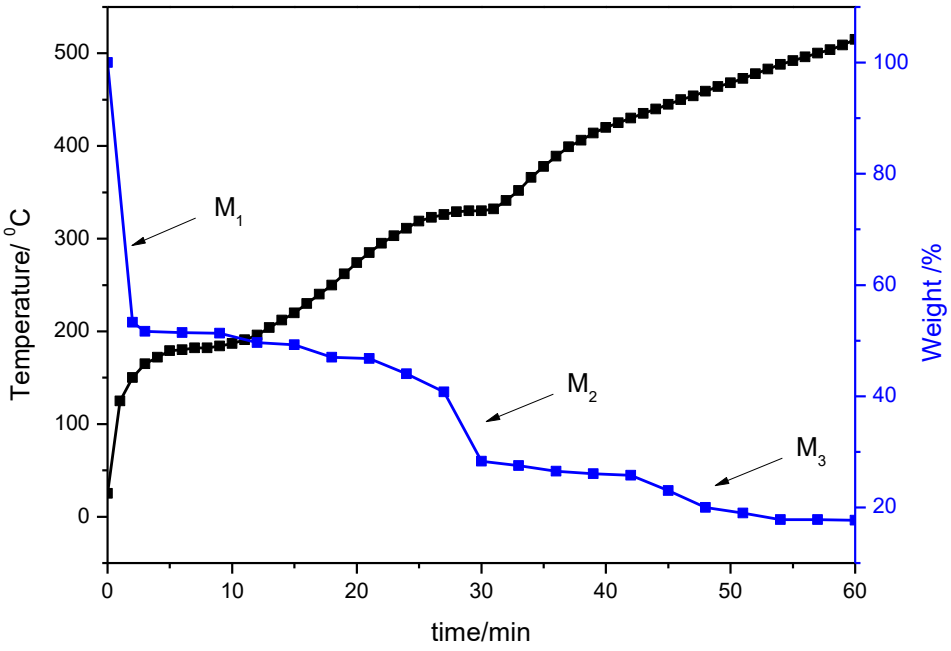

Figure 1. Curves of temperature-rising and mass loss of $[BMIm]N(CN)_2$ during microwave irradiation

The ionic liquid $[BMIm]N(CN)_2$ has high dipole moments and thus can be heated rapidly under microwave irradiation[30]. The temperature of $[BMIm]N(CN)_2$ reached 150 °C after microwave irradiated for 2 minutes, resulting in the first mass loss (M_1) of 46.6%. It was mainly caused by the decomposition of methyl and butyl groups. The second mass loss M_2, appeared in the range of 320-330 °C, was due to the carbonization of $[BMIm]N(CN)_2$. The third mass loss was caused by the loss of nitrogen in the nitrogen-doped carbon product. The residue material which held 17.8 % of the original mass was the nitrogen-doped carbon.

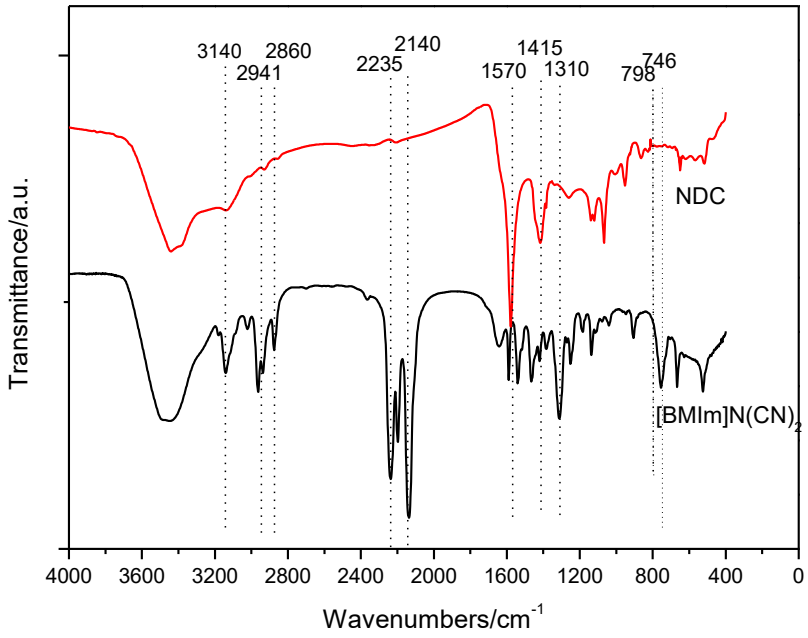

Figure 2. FT-IR spectra of $[BMIm]N(CN)_2$ and NDC

FT-IR test was performed on the pristine $[BMIm]N(CN)_2$ and the pyrolysis product NDC (Figure 2). As expected, the characteristic peaks of pristine $[BMIm]N(CN)_2$ showed in the range of 746 cm^{-1} to 3140 cm^{-1}. The peak at 3140 cm^{-1} was attributed to the stretching vibrations of aromatic C-H. The peaks at 2941cm^{-1}, 2860cm^{-1} and 1310cm^{-1} corresponded to the asymmetric and symmetric stretching vibrations of aliphatic C-H bonds[31]. The peak at 746cm^{-1} was caused by the deformation of C-H bonds. The typical peaks at 2235cm^{-1} and 2140cm^{-1} were ascribed to the stretching vibrations of C≡N in the anion $N(CN)_2^-$. The broad peak at about 3500 cm^{-1} arose from the absorbed moisture[32].

The transmittance of the characteristic peaks of NDC were greatly reduced from that of the pristine $[BMIm]N(CN)_2$ at 3140 cm^{-1}, 2941 cm^{-1}, 2860 cm^{-1}, 2235 cm^{-1}, 2140 cm^{-1}, 1310 cm^{-1} and 746 cm^{-1}, indicating the decomposition of methyl and butyl groups and the break of C≡N chemical bonds. Nevertheless, several new absorption peaks appeared at 798cm^{-1} and in the range of 1200cm^{-1} to 1700cm^{-1}. The absorptions between 1200cm^{-1} and 1700cm^{-1} were attributed to the stretching vibrations of triazine ring and the sharp absorption at 798cm^{-1} belonged to deformation of triazine rings[33] .

The XRD pattern of the pyrolysis product NDC was shown in Figure 3(a). NDC possessed sharp peaks at 2θ of 27^0, explaining that the obtained nitrogen-doped carbon had a graphite structure[34]. This result was agreed well with the result of Raman Spectra.

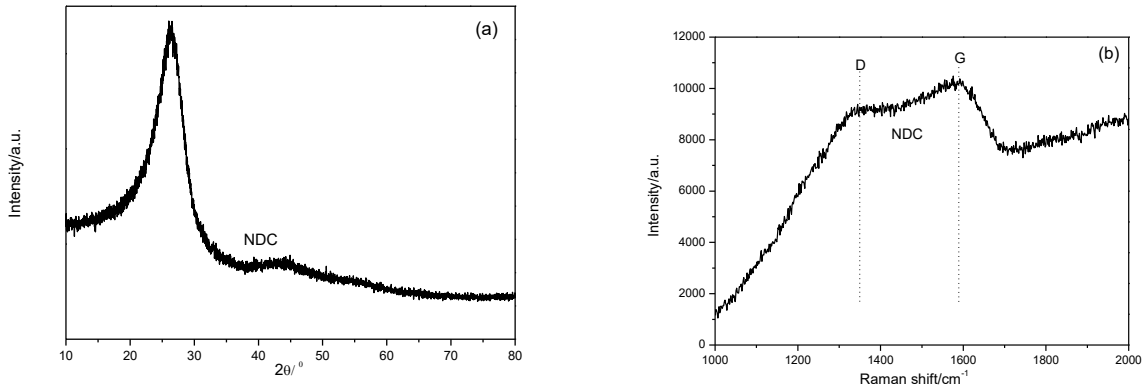

Figure 3. XRD pattern (a), Raman spectra (b) of NDC

The Raman spectra of NDC was shown in Figure 3(b). Two broaden peaks at 1350cm^{-1} and 1570 cm^{-1} were corresponded to the D and G bands, respectively[35].

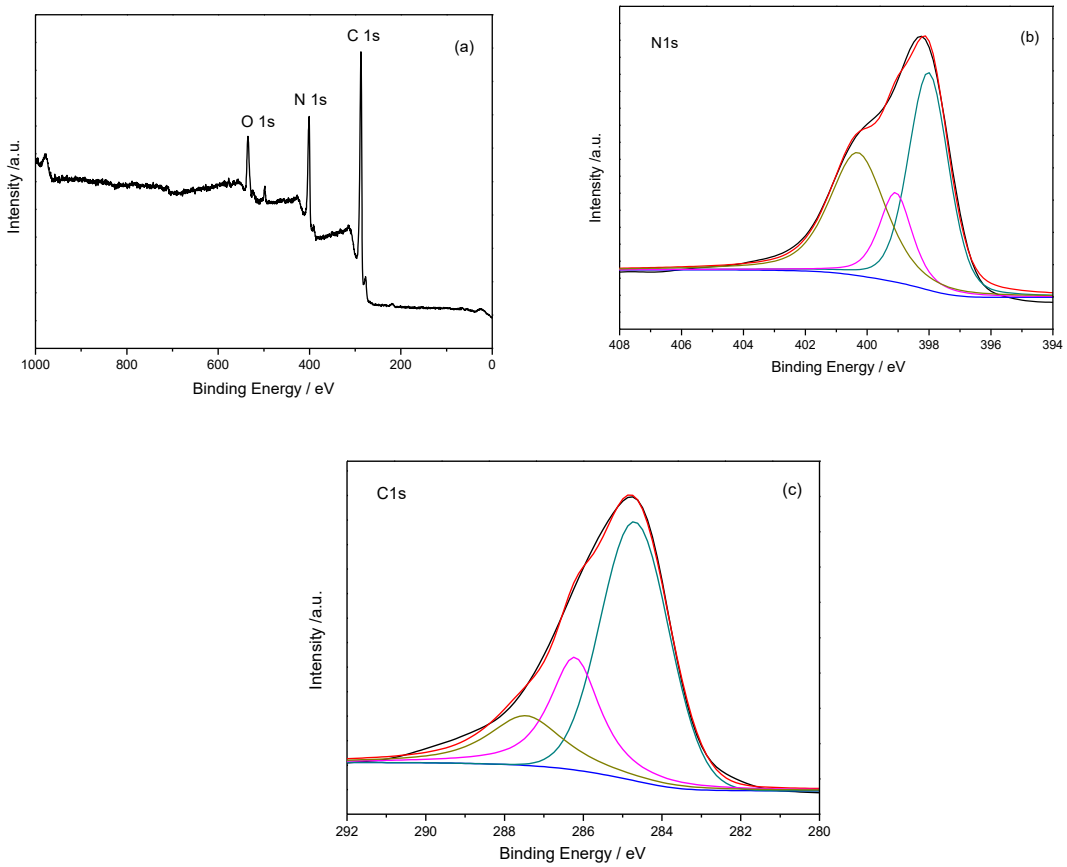

Figure 4. XPS survey spectrum (a), High-resolution N1s (b) and C1s spectra (c) of NDC

The G band was attributed to the E_{2g} vibration mode that was present due to the sp^2 bonded graphitic carbons[36, 37]. The disorder degree of graphite crystal structure of carbon materials can be

characterized by the relative intensity of D band between 1200 cm^{-1} and 1450 cm^{-1}. The disorder degree of carbon materials can also be evaluated by the intensity ratio of D band to G band[38, 39]. The higher of the I_D/I_G ratio, the lower the degree of graphitization of the carbon products[40]. The D band and G band of NDC in Figure 3(b) was fitted and the values of I_D/I_G was calculated as 1.015, indicating a large number of defects in the nitrogen-doped carbon products, which could serve as the reaction site of Li^+ ion adsorption.

The XPS survey spectrum of the NDC was shown in Figure 4. The element C, N and O could be easily identified by their characteristic peak of C1s, N1s and O1s, respectively. The fine N1s spectrum (Figure 4(b)) of the NDC indicated three kinds of nitrogen doping, of which the pyridinic N, pyrrolic N, and graphitic N were shown by peaks at 398.4eV, 399.1eV, and 400.8eV, respectively[1, 2]. The fine C1s spectrum (Figure 4(c)) also indicated the existence of N. The peaks at 284.6, 286.0 and 287.6eV can be assigned to graphitic C, C=N, and C-N groups, respectively[41, 42] . Moreover, the dominance of the graphitic C peak in Figure 4(c) suggested that the NDC possess a graphitic structure, while the large portion of the C-N/C=N peak indicated a strong nitrogen doping, which may create a large number of defects and introduce many sites that are active for the Li^+ ion adsorption.

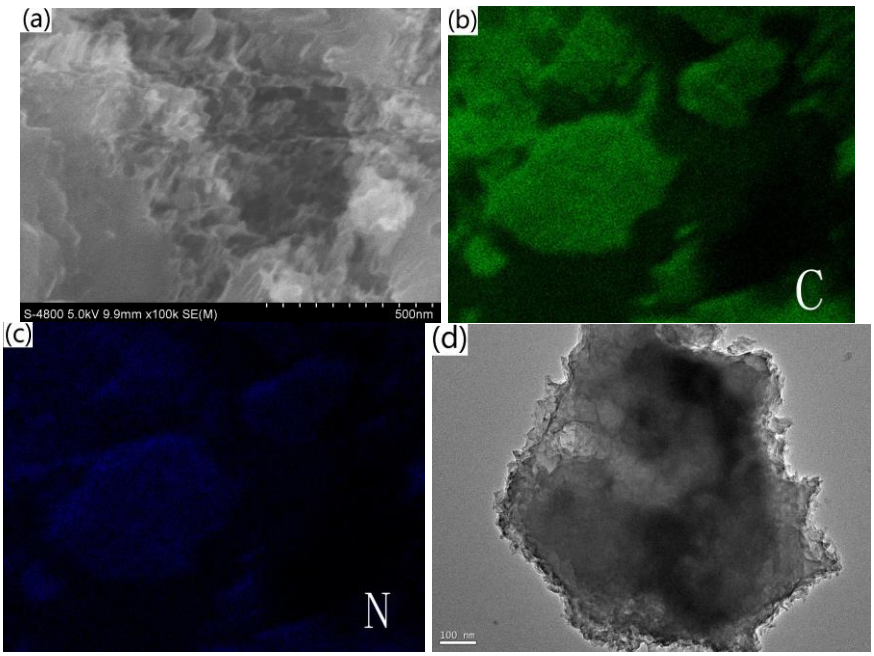

Figure 5. SEM image (a), EDS map for Carbon (b), EDS map for Nitrogen(c) and TEM image (d) of NDC

The electron microscopy was applied to observe the morphology of the NDC. As shown in Figure 5 (a), the as-prepared NDC shows network morphology of lamellar structure. Figure 5(b) and 5(c) indicates that element nitrogen is uniformly dispersed in the NDC, which is essential to improve the electric conductivity of NDC[8, 43, 44]. The TEM image (Figure 5 (d)) further reveals many pores and defects in the NDC, caused by the nitrogen doping in the carbon matrix. The obtained NDC possessed large surface area of S_{BET}=191.3 m^2/g.

The electrochemical performances of the NDC were shown in Figure 6.The first three discharge–charge profiles of the NDC at 0.2C (1C = 372.0 $mA.g^{-1}$), were shown in Figure 6(a). Obviously, a difference between the first and the subsequent cycles in the discharge-charge curves was observed. The discharge specific capacity of the NDC at the first cycle reached 1088.1$mAhg^{-1}$.The plateau at about 0.5V in the first cycle was attributed to the formation of the solid electrolyte interphase (i.e. SEI) layer on the surface of the NDC. The formation of the SEI layer caused the large initial irreversible capacity.

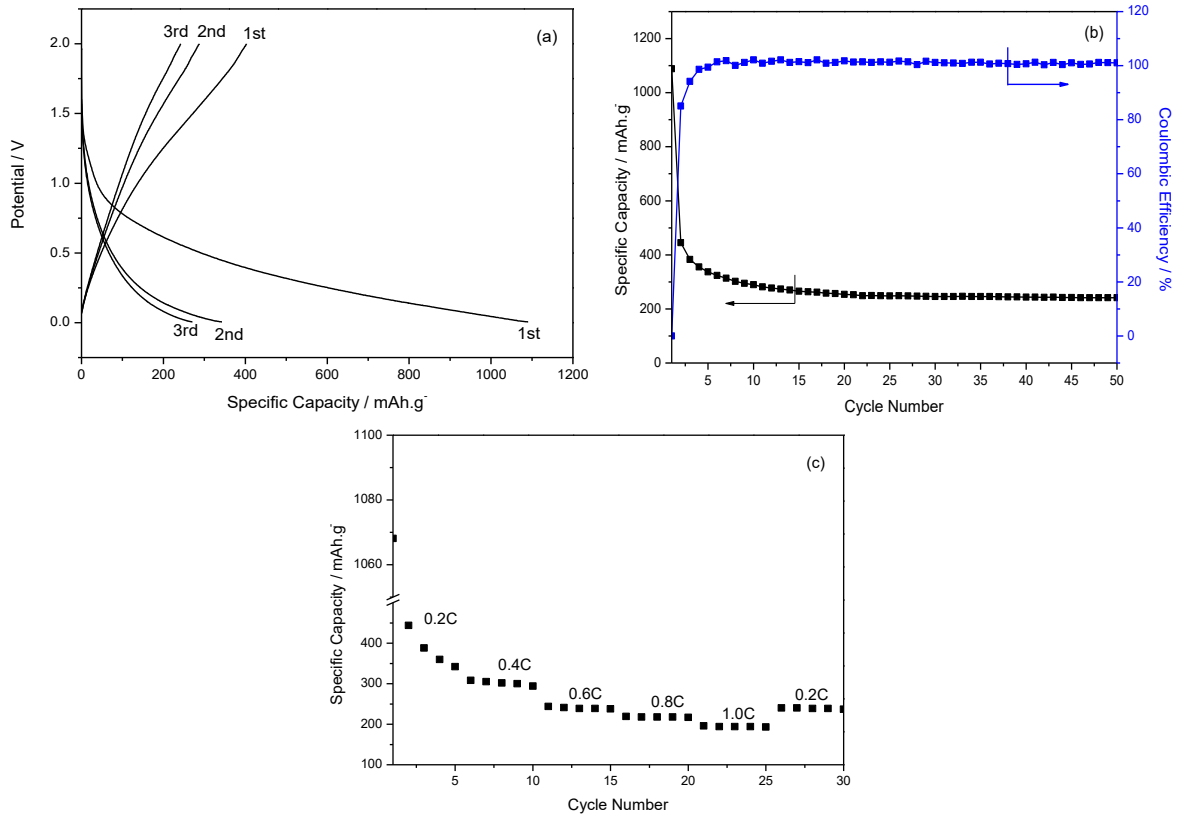

Figure 6. First three charge/discharge curves (a), Cycling performances (b) and Rate capability at different current density(c) of the NDC

Figure 6(b) and 6(c) showed that the NDC delivered a specific capacity of 243.6$mAh.g^{-1}$ after 50 cycles at 0.2C and 196$mAh.g^{-1}$ after 50 cycles at 1.0C. The NDC had improved lithium storage performance because of its better electrode/electrolyte wettability, high electronic conductivity and structure stability for lithium storage[2, 4, 7]. In addition, the large number of defects and edge sites in the nitrogen-doped carbon were beneficial to the lithium storage performance [9].

4. CONCLUSIONS

Nitrogen-doped carbon nanosheet (NDC) was prepared by microwave-assisted pyrolysis of ionic liquid $[BMIm]N(CN)_2$. Owning to the high dipole moments of $[BMIm]N(CN)_2$, it can be heated

rapidly under microwave irradiation. The obtained nitrogen-doped carbon originated mainly from the anion $N(CN)_2^-$ and possessed a graphite structure. Doping with nitrogen atoms can improve the electric conductivity of carbon materials. In addition, the nitrogen dopant in NDC created a porous structure and a large number of defects. The pores and defects in the surfaces of NDC introduced many sites that were active for the Li^+ ion adsorption. The specific capacity of the NDC reached 1088.1mAhg^{-1} at the first cycle and remained 243.6mAh.g^{-1} after 50 cycles at 0.2C. Even at a high current rate of 1.0C, the NDC still delivered a reversible capacity of 196mAh.g^{-1} after 50 cycles when used as anode for lithium ion batteries.

CONFLICTS OF INTEREST STATEMENT

The authors certify that they have NO affiliations with or involvement in any organization or entity with any financial interest (such as honoraria; educational grants; participation in speakers' bureaus; membership, employment, consultancies, stock ownership, or other equity interest; and expert testimony or patent-licensing arrangements), or non-financial interest (such as personal or professional relationships, affiliations, knowledge or beliefs) in the subject matter or materials discussed in this manuscript.

ACKNOWLEDGEMENT

The project was supported by the National Natural Science Foundation of China (grant No. 51364024, 51404124), Natural Science Foundation of Gansu Province (grant No. 1506RJZA100), Research and Development Fund of Lanzhou University of Technology (01-0443).

References

1. X.B. Cheng, Q. Zhang, H.F. Wang, G.L. Tian, J.Q. Huang, H.J. Peng, M.Q. Zhao, F. Wei, *Catal Today*, 249 (2015) 244.
2. X.W. Liu, Y. Wu, Z.Z. Yang, F.S. Pan, X.W. Zhong, J.Q. Wang, L. Gu, Y. Yu, *J Power Sources*, 293 (2015) 799.
3. Y.M. Li, X.J. Lv, J. Lu, J.H. Li, *J Phys Chem C*, 114 (2010) 21770.
4. Z.Q. Jiang, Z.J. Jiang, X.N. Tian, L.J. Luo, *Electrochim Acta*, 146 (2014) 455.
5. B. Qiu, C.T. Pan, W.J. Qian, Y.J. Peng, L.H. Qiu, F. Yan, *J Mater Chem A*, 1 (2013) 6373.
6. M.J. Zhi, C.C. Xiang, J.T. Li, M. Li, N.Q. Wu, *Nanoscale*, 5 (2013) 72.
7. W. Ren, D.J. Li, H. Liu, R. Mi, Y. Zhang, L. Dong, L. Dong, *Electrochim Acta*, 105 (2013) 75.
8. L. Qie, W.M. Chen, Z.H. Wang, Q.G. Shao, X. Li, L.X. Yuan, X.L. Hu, W.X. Zhang, Y.H. Huang, *Adv Mater*, 24 (2012) 2047.
9. X.L. Li, H.L. Wang, J.T. Robinson, H. Sanchez, G. Diankov, H.J. Dai, *J Am Chem Soc*, 131 (2009) 15939.
10. J.P. Dong, X.M. Qu, L.J. Wang, C.J. Zhao, J.Q. Xu, *Electroanal*, 20 (2008) 1981.
11. H.Y. Jin, N.C. Bing, L.L. Wang, L.J. Wang, *Mater Sci Forum*, 694 (2011) 266.
12. D. Higgins, Z. Chen, Z.W. Chen, *Electrochim Acta*, 56 (2011) 1570.
13. C.S. Shan, W.J. Zhao, X.L. Lu, D.J. O'Brien, Y.P. Li, Z.Y. Cao, A.L. Elias, R. Cruz-Silva, M. Terrones, B.Q. Wei, J. Suhr, *Nano Lett*, 13 (2013) 5514.
14. W.F. Chen, F.S. Cannon, and J.R. Rangel-Mendez, *Carbon*, 43 (2005) 573.
15. B.L. Allen, M.B. Keddie, A. Star, *Nanoscale*, 2 (2010) 1105.
16. M.H. Wu, X. Li, D. Pan, L. Liu, X.X. Yang, Z. Xu, W.L. Wang, Y. Sui, X.D. Bai, *Chinese Phys B*,

22 (2013).
17. G.Q. Ning, C.G. Xu, X. Zhu, R.F. Zhang, W.Z. Qian, F. Wei, Z.J. Fan, J.S. Gao, *Carbon*, 56 (2013) 38.
18. G.K. Goswami, R. Nandan, K.K. Nanda, *Carbon*, 56 (2013) 97.
19. P. Ayala, A. Grüneis, T. Gemming, D. Grimm, C. Kramberger, M.H. Rümmeli, F.L. Freire, H. Kuzmany, R. Pfeiffer, A. Barreiro, *J Phys Chem C*, 111 (2007) 2879.
20. W.Z. Shen, W.B. Fan, *J Mater Chem A*, 1 (2013) 999.
21. X.Q. Wang, S. Dai, *Angew Chem Int Edit*, 49 (2010) 6664.
22. J.S. Lee, X.Q. Wang, H.M. Luo, G.A. Baker, S. Dai, *J Am Chem Soc*, 131 (2009) 4596.
23. L.J. Zhi, Y.S. Hu, B. El Hamaoui, X. Wang, I. Lieberwirth, U. Kolb, J. Maier, K. Mullen, *Adv Mater*, 20 (2008) 1727.
24. P.F. Fulvio, J.S. Lee, R.T. Mayes, X.Q. Wang, S.M. Mahurin, S. Dai, *Phys Chem Chem Phys*, 13 (2011) 13486.
25. J.P. Paraknowitsch, A. Thomas, *Macromol Chem Phys*, 213 (2012) 1132.
26. J.S. Lee, X. Wang, H. Luo, S. Dai, *Adv Mater*, 22 (2010) 1004.
27. A.M. Schwenke, S. Hoeppener, U.S. Schubert, *Adv Mater*, 27 (2015) 4113.
28. C.O. Kappe, D. Dallinger, S.S. Murphree, Practical Microwave Synthesis for Organic Chemists: Strategies, Instruments, and Protocols, 2009.
29. Y. Meng, Z. Zhang, W. Han, Y. Zhang, F. Zhu, D. Wang, *NANO*, (2015) 1650004.
30. S. Mallakpour, Z. Rafiee, *Prog Polym Sci*, 36 (2011) 1754.
31. D.L. Xiao, D.H. Yuan, H. He, M.M. Gao, *J Lumin*, 140 (2013) 120.
32. S. Vadahanambi, J.H. Jung, R. Kumar, H.J. Kim, I.K. Oh, *Carbon*, 53 (2013) 391.
33. D. Foy, G. Demazeau, P. Florian, D. Massiot, C. Labrugere, G. Goglio, *J Solid State Chem*, 182 (2009) 165.
34. Z.H. Tang, Y. Song, X. He, J.H. Yang, *Mater Lett*, 89 (2012) 330.
35. A. Ferrari, J. Meyer, V. Scardaci, C. Casiraghi, M. Lazzeri, F. Mauri, S. Piscanec, D. Jiang, K. Novoselov, S. Roth, *Physical review letters*, 97 (2006) 187401.
36. P.X. Han, Y.H. Yue, L.X. Zhang, H.X. Xu, Z.H. Liu, K.J. Zhang, C.J. Zhang, S.M. Dong, W. Ma, G.L. Cui, *Carbon*, 50 (2012) 1355.
37. M.S. Dresselhaus, G. Dresselhaus, R. Saito, A. Jorio, *Physics Reports*, 409 (2005) 47.
38. M. Nakamizo, R. Kammereck, P.L. Walker, *Carbon*, 12 (1974) 259.
39. B. Yen, *Carbon*, 34 (1996) 489.
40. L. Zou, B. Huang, Y. Huang, Q. Huang, C.A. Wang, *Materials Chemistry & Physics*, 82 (2003) 654.
41. J.K. Meng, Y. Suo, J. Li, G.P. Zheng, Y.S. Liu, J.M. Zhang, X.C. Zheng, *Mater Lett*, 160 (2015) 392.
42. K.L. Zhang, X.N. Li, J.W. Liang, Y.C. Zhu, L. Hu, Q.S. Cheng, C. Guo, N. Lin, Y.T. Qian, *Electrochim Acta*, 155 (2015) 174.
43. J.P. Paraknowitsch, A. Thomas, M. Antonietti, *J Mater Chem*, 20 (2010) 6746.
44. B. Xu, S.S. Hou, G.P. Cao, F. Wu, Y.S. Yang, *J Mater Chem*, 22 (2012) 19088.